

The Mechanical Properties of Thin Polycrystalline Silicon Films as Function of Deposition and Doping Conditions

Lüder Elbrecht* and Josef Binder

Institute for Microsensors, Actuators, and Systems (IMSAS)
University of Bremen, D-28334 Bremen, Germany

(Received November 4, 1998; accepted February 1, 1999)

Key words: polycrystalline silicon, surface micromachining, stress, Young's modulus, Poisson's ratio, fracture strength, doping, annealing

Polycrystalline silicon (polysilicon) has become the favorite thin-film material for the fabrication of integrated micromechanical sensors and actuators in the past decade. On the one hand, its excellent mechanical properties and the well-developed polysilicon deposition and patterning technology in microelectronics processing make the material an ideal candidate for a variety of micromechanical applications. On the other hand, the mechanical characteristics of polysilicon thin films may vary within a wide range depending on the deposition, doping and other postprocessing parameters. Thus, a fundamental understanding of these relationships is necessary to develop optimized processing sequences for free-standing microstructures. In this paper, the correlation of processing parameters during deposition and doping with the mechanical film properties is comprehensively discussed. It is shown how deposition and doping parameters cause changes in grain formation, microstructure and surface roughness of the polycrystalline thin films, which, in turn, cause changes in elastic properties, film stress and fracture strength.

1. Introduction

The advantages of silicon as a mechanical material were already outlined in the outstanding paper of Petersen in 1982.⁽¹⁾ In the same year, Howe and Muller at the University of California, Berkeley, demonstrated for the first time the opportunity of using thin polycrystalline silicon (polysilicon) films for the fabrication of micromechanical

*Present address: Siemens AG – Semiconductor Group, HL GS SNS/MchB 10629, P.O. Box 80 17 09, D-81617 Muenchen, Germany

structures.^(2,3) These films combine the excellent mechanical properties of silicon with the patterning simplicity and flexibility of thin-film technology. The papers of the Berkeley group represented the rebirth of surface micromachining technology, approximately twenty years after the first attempts had been made by Nathanson and Wickstrom using thin metal films.⁽⁴⁾ Nowadays, majority of the micromechanical products are fabricated using polycrystalline silicon as the mechanical material.⁽⁵⁻⁷⁾

However, the crystalline microstructure of these films — and thus their mechanical properties — may vary within a wide spectrum depending on the deposition parameters and the subsequent doping and annealing processes. Although deposition processes optimized for the use in micromechanical applications have been presented in the past,⁽⁸⁻¹¹⁾ the fundamental dependences are not yet fully understood.

In this paper, the relationship between processing conditions and the mechanical properties of thin polycrystalline silicon films is comprehensively discussed. In this context, new experimental results are presented to strengthen the described dependences. As the mechanical properties of undoped films may differ markedly from those of highly doped films, these two cases are discussed separately.

2. Undoped Polysilicon Films

2.1 Microstructure

For polysilicon films fabricated by low-pressure chemical vapor deposition (LPCVD), two different growth mechanisms are found.^(12,13) For films deposited at temperatures above 610°C, crystalline grain growth is observed. In this case, the grain formation can be divided into two steps. In the first step, randomly oriented nuclei grow until the forming grains collide (*coalescence*). The density of these grains decreases with increasing deposition temperature and decreasing silane-partial-pressure.⁽¹⁴⁻¹⁶⁾ Typical grain diameters are in the range of 50 nm to 100 nm. After the coalescence, grain growth can only continue in the direction normal to the substrate surface, whereby (due to the different growth rates of silicon in different crystallographic directions) columnar grains with a preferred grain orientation are formed. The preferred grain orientation is typically {110},^(17,18) although {100} and {311} textures have also been found under certain deposition conditions. The cross-sectional view of a polysilicon film deposited at 620°C is shown in Fig. 1(a). The deposition (as all other deposition-processes discussed in this paper) was carried out with a gas-flow of 80 sccm of pure silane at a pressure of 200 mTorr.

For deposition temperatures below 560°C, the deposited films are typically fully amorphous (Fig. 1(b)). When these films are crystallized in a subsequent annealing step, randomly oriented grains are formed (Fig. 1(d)). For films deposited in the temperature range between 560°C and 600°C, this crystallization partly takes place already during the deposition process itself. In this case, the bottom part of the film is already crystalline after deposition, while the most recently deposited top part of the film is still amorphous (Fig. 1(c)). Comparing only films that were fully crystallized in an annealing step following the deposition, no significant differences in the microstructure were found for films deposited in the temperature range between 560°C and 590°C.

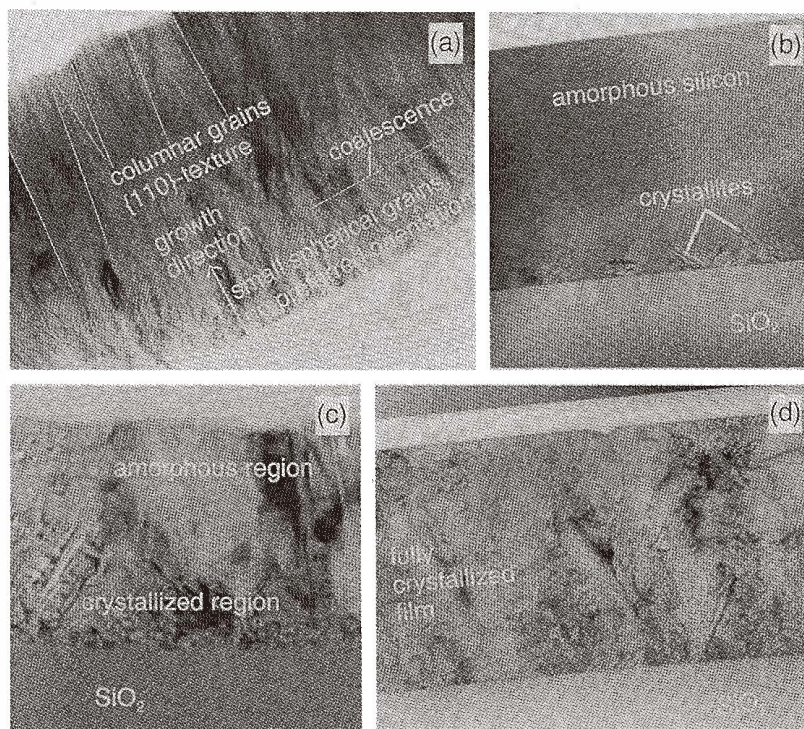


Fig. 1. Cross-sectional TEM images of LPCVD-silicon films obtained for different deposition temperatures. (a) Polycrystalline grain growth at 620°C. (b) Nearly fully amorphous film deposited at 565°C. (c) Partially crystallized film deposited at 580°C. (d) Film deposited at 565°C and fully crystallized at 650°C. The thickness is approximately 500 nm for all films.

2.2 Young's modulus and Poisson's ratio

Due to the varying elastic properties of single crystalline silicon for different crystallographic planes,⁽¹⁹⁾ Young's modulus E and Poisson's ratio ν are expected to vary with the dominant grain orientation in polycrystalline silicon films. In this paper, only the in-plane elastic properties are discussed. For randomly oriented grains, $E = 163$ GPa and $\nu = 0.223$ are predicted, whereas for a pronounced $\{110\}$ film texture, $E = 166$ GPa and $\nu = 0.229$.⁽²⁰⁻²²⁾ As discussed above, films that are deposited directly in the polycrystalline state have randomly oriented grains on the bottom and $\{110\}$ -textured grains on top, therefore, should show values between these two limits. As only the textured part of the film increases with increasing film thickness, thick films are expected to show a higher Young's modulus and Poisson's ratio. On the other hand, films that are deposited in the amorphous form and subsequently crystallized have randomly oriented grains; thus they should not show any thickness dependence. However, such small variations of the elastic moduli of

thin films are hard to detect experimentally with sufficient accuracy; we measured $E = (170 \pm 20)$ GPa for both polycrystalline and amorphously deposited films using micromachined test structures.⁽²³⁾ These structures have indicators with a deflection proportional to film stress and inversely proportional to Young's modulus. If film stress can be determined by an independent method (*e.g.* wafer-bow-measurement), and both stress and Young's modulus are not influenced by the patterning process of the microstructure, the elastic modulus can be extracted. The results reported by other authors using other measurement methods are similarly close to the expected values for $\{110\}$ -textured^(22,24-26) and randomly oriented films.^(22,27,28)

2.3 Film stress and intrinsic bending moment

Regarding the origin of stress in undoped polycrystalline silicon films, two major contributions have to be taken into account. First, compressive stress originates during the formation of grain boundaries.⁽¹⁸⁾ This contribution increases with increasing grain density (*i.e.* decreasing grain diameter). Due to this, polycrystalline silicon typically exhibits a large compressive stress at the bottom and a smaller compressive stress in the textured top part of the film (Fig. 2, plot A). This unbalanced stress distribution within the film generates an intrinsic bending moment, causing an upward bending of the released microstructures. The second contribution to intrinsic film stress has to be considered for films that are deposited amorphously and subsequently crystallized. Film shrinkage due to the higher package density of the crystalline state causes tensile stress. Before crystallization, these films are also compressive (Fig. 2, plot B), due to the lower thermal expansion coefficient of amorphous silicon. Depending on the density of the amorphous layer, the overall stress in the crystallized films is typically tensile (Fig. 2, plot C). We found no differences in the stress state for films that were deposited in the temperature range between 565°C and 595°C and subsequently crystallized at 650°C (Fig. 3). This indicates that there are no significant changes in the density of the amorphous film with regard to the deposition temperature within the investigated range of deposition temperature. Due to the constant stress distribution, the intrinsic bending moment is small for these films.

The presented results are in good agreement with the results reported by other authors,⁽²⁹⁻³²⁾ which leads us to the conclusion that other presumed stress contributions, including thermal mismatch to single crystalline silicon and the incorporation of foreign atoms during deposition, are of little importance. Nevertheless, high quantities of foreign atoms (*e.g.* oxygen) can effectively change polysilicon film stress.⁽³³⁾

2.4 Fracture strength

Although it is known that the fracture of polysilicon is not determined by the grain boundaries,⁽³⁴⁾ it is strongly affected by surface roughness,⁽³⁵⁾ which itself is correlated to the grain growth mechanism. Figure 4 shows the surface topology of films deposited at 620°C and 585°C (with subsequent crystallization). The amorphously deposited film is smoother than the film deposited at 620°C, and the smoothest surfaces are achieved for films with no crystallization during film deposition (compare with Fig. 1(d)). Thus, the highest tensile strength is expected for films with low deposition temperatures. Additionally, the observed average value of the fracture stress is known to increase with decreasing

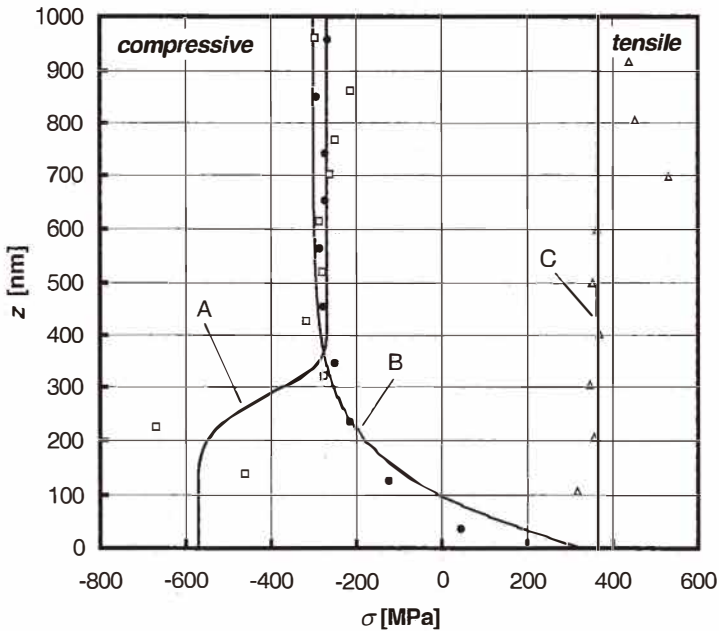


Fig. 2. Stress profile in 1- μm -thick polysilicon films after deposition (plots A and B) and crystallization (plot C). Plot A is for the film deposited at 620°C. The other two plots show the stress profile in a film deposited at 565°C before (plot B) and after (plot C) crystallization at 650°C. Before crystallization, the film is only tensile at the bottom part due to crystallization during the deposition process (compare with Fig. 1(b)). The stress was determined from wafer-bow measurements. The accuracies are 5 MPa for the film stress and 100 nm for the film thickness measurements.

specimen size.⁽³⁶⁾ We used a set of micromachined test beams smaller than $4\ \mu\text{m} \times 1\ \mu\text{m}$ for the investigation of fracture strength (see Fig. 5). The test beams are clamped by two wider beams, which multiply the film stress by a factor defined by the ratio of widths and lengths of the test beams and the wider beams.⁽³⁵⁾ The test specimens have intentionally rounded edges to minimize influences from the patterning process. Figure 6 shows a measured fracture-probability-curve for a 500-nm-thick polysilicon film deposited at 585°C and crystallized at 650°C with a mean fracture strength of 4 GPa. This indicates that the fracture toughness of smooth polysilicon films approaches the value of single crystalline silicon, which is found to be in the range of 3 to 7 GPa.⁽³⁷⁻⁴⁰⁾

2.5 Postprocessing

Undoped polycrystalline films are relatively stable during postdeposition annealing. Noticeable change in grain structure is not observed until annealing temperatures above

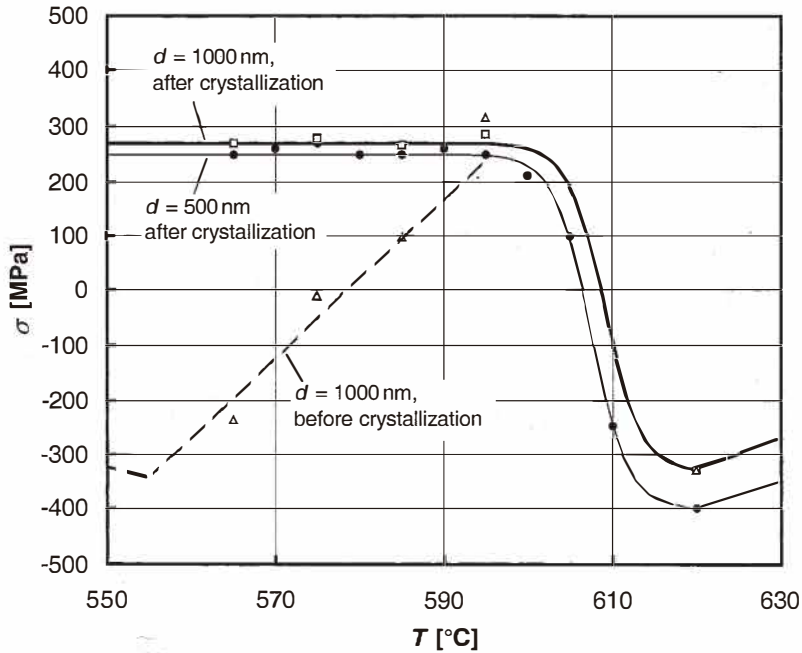


Fig. 3. Overall stress in polycrystalline silicon films deposited in the temperature range between 550°C and 630°C. The difference in stress without and with postdeposition crystallization (650°C in nitrogen ambient) is shown for the 1- μm -thick films.

1,000°C.^(16,22,41) Thus, no substantial changes in elastic properties and film stress are found for undoped polysilicon films using the usual high-temperature postprocessing steps. This is not the case for highly doped polysilicon films.

3. Doped Polysilicon Films

The mechanical properties of thin polysilicon films are affected in two ways by doping: On the one hand, the dopant atoms themselves may contribute to intrinsic film stresses. On the other hand, doping and the associated annealing processes are typically accompanied by substantial recrystallization and grain growth effects, which alter the mechanical behavior of the film. The latter effect is typically the dominant factor.

3.1 Microstructure

Looking at recrystallization effects and grain growth promoted by doping, *n*- and *p*-type dopants have to be discriminated. *n*-Type dopants such as phosphorus and arsenic are known to accumulate heavily at the grain boundaries, thus increasing the tendency of grain reformation.⁽⁴²⁻⁴⁴⁾ In this study, only phosphorus doping is investigated. However,

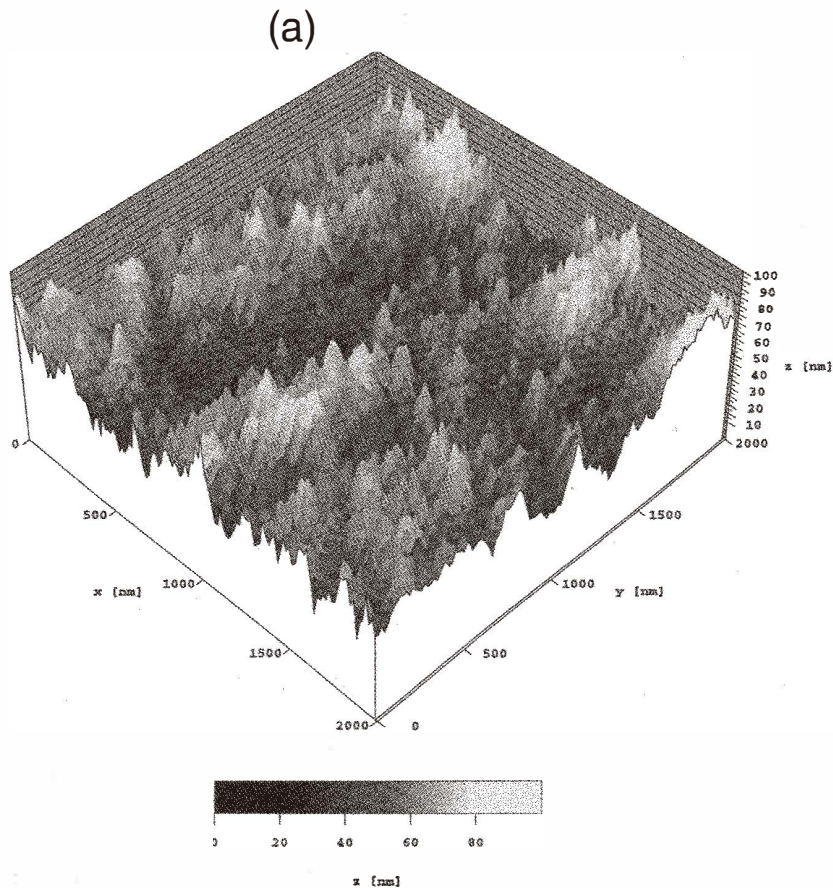


Fig. 4(a). Surface roughness of undoped polycrystalline silicon films measured using an atomic force microscope (AFM). (a) Film deposited at 620°C.

comparable results have been found for arsenic-doped films.⁽⁴⁵⁻⁴⁷⁾ For *p*-type dopants, the recrystallization effects are less pronounced due to the lack of grain boundary dopant accumulation.⁽⁴⁸⁾

The changes in crystalline microstructure due to doping and subsequent annealing can be subdivided into two successive steps.⁽¹³⁾ In the first step (*primary recrystallization*), new nuclei are formed in the already crystalline film. The recrystallized grains being formed are nearly free of defects and can have diameters similar to the film thickness. Figure 7 shows two films with different deposition conditions after recrystallization during phosphorus diffusion doping at 950°C (phosphorus concentration larger than 5×10^{20} atoms/cm³). It can be seen that for the film deposited at 620°C (Fig. 7(a)), the two regions

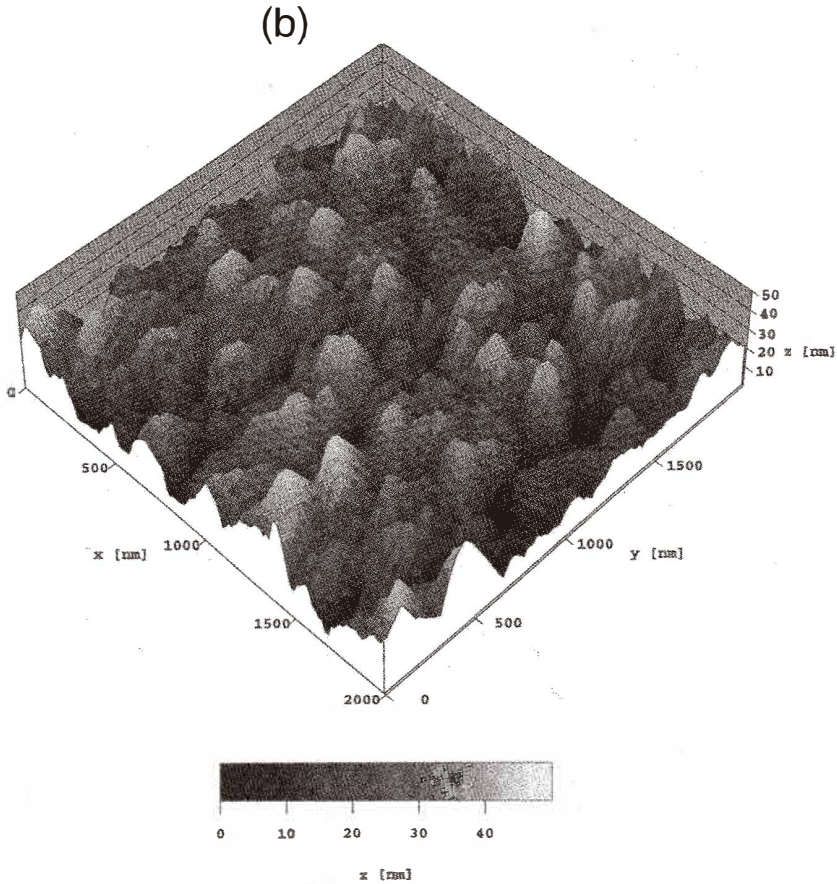


Fig. 4(b). Surface roughness of undoped polycrystalline silicon films measured using an atomic force microscope (AFM). (b) Film deposited at 585°C and crystallized at 650°C in a nitrogen ambient directly after deposition.

of grain growth during deposition also lead to two separated regions of recrystallization. Because of the random orientation of the nuclei, the grains formed during primary recrystallization have no preferred orientation.

If fully recrystallized films are exposed to further high-temperature treatments, an anomalous grain growth (also called *secondary recrystallization*) takes place. As the growth rate of silicon depends on crystal direction, the grain growth by diffusion of single silicon atoms across the grain boundaries depends on the orientation of the singular grains within the film plane. Grains with rapidly growing planes perpendicular to the film surface are growing to the disadvantage of surrounding grains with slower growing crystal planes

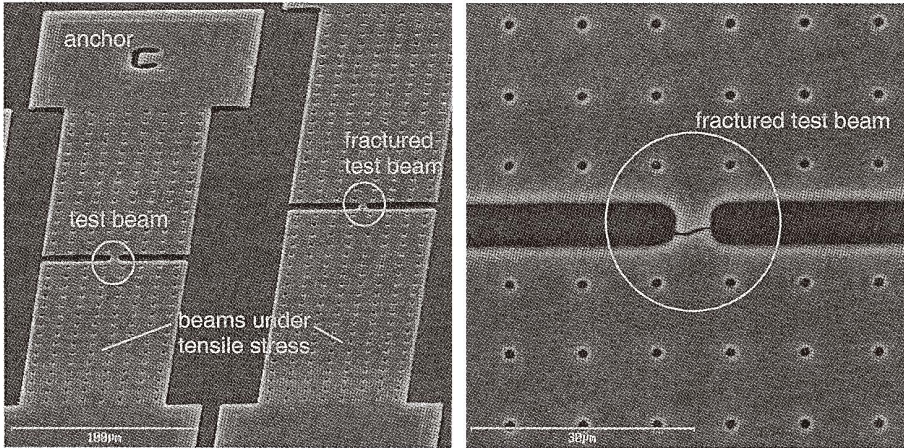


Fig. 5. SEM images of the test structure used for fracture strength determination.

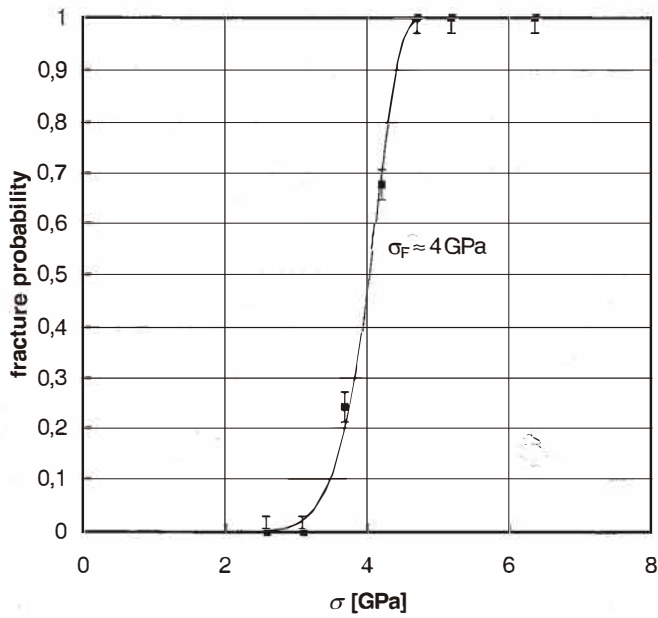


Fig. 6. Experimentally determined fracture probability curve for a 500-nm-thick polysilicon film.

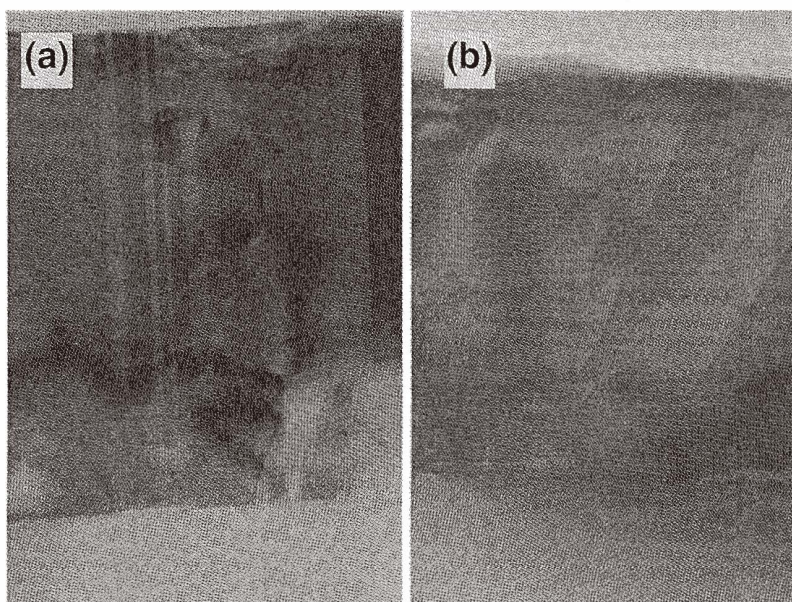


Fig. 7. Cross-sectional TEM images of phosphorus-doped polysilicon films deposited at (a) 620°C and (b) 585°C. The doping is done by POCl_3 diffusion at 950°C.

in the same direction. The grains that grow during secondary recrystallization (anomalous grain growth) are therefore highly textured, with the texture being $\{111\}$. If the secondary grain growth is not completed, a bimodal grain size distribution is found, where the diameter of the larger grains can be much greater than the film thickness itself.

3.2 *Young's modulus and Poisson's ratio*

Due to the change in preferred grain orientation, Young's modulus and Poisson's ratio may be substantially changed by doping and subsequent annealing processes. The changes expected by the dominant film texture are summarized in Fig. 8. However, the scattering of the experimental data is still too large to prove that other doping-induced effects may be neglected.^(24,27,28,49,50)

3.3 *Film stress and intrinsic bending moment*

The most pronounced effect of doping on polysilicon film stress is the reduction of strain energy during the recrystallization processes. Thus, recrystallized films typically have a very low stress level. As recrystallization is intensified by higher dopant concentrations (for *n*-type dopants) and a higher annealing temperature, lower stress levels can be achieved within the same annealing time by increasing these two parameters. However, for fully recrystallized and highly phosphorus-doped films, a small compressive residual stress is observed. This behavior is illustrated in Fig. 9. It is assumed that this compressive

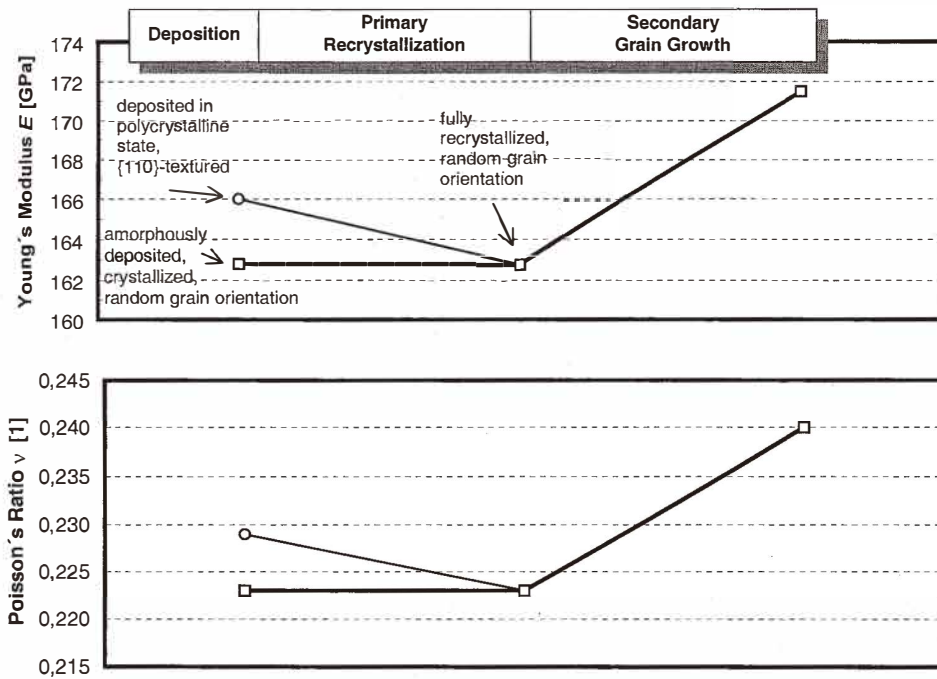


Fig. 8. Change of the elastic properties of polysilicon films by doping and subsequent annealing as expected from the change in film texture (calculation).

contribution is generated by the excess phosphorus atoms that are forced away from the former grain boundaries.⁽¹⁶⁾ For films doped in an oxidizing ambient (such as POCl_3 diffusion), the enhanced oxidation of the grain boundaries is found to be an additional source of compressive film stress. Due to the dependence of stress relaxation on dopant concentration, a uniform dopant profile (or at least a symmetric one) throughout the film thickness is necessary to maintain a small stress gradient associated with a low intrinsic bending moment. Thus, *in situ* doping and doping by ion implantation are superior to diffusion doping methods (*e.g.*, from PSG or POCl_3).

3.4 Fracture strength

The recrystallization processes are also accompanied by changes in the surface roughness of the polysilicon films,⁽⁵¹⁾ thus causing changes in the fracture strength of the films. As shown in Fig. 10, recrystallized films are typically smoother than undoped films deposited in the polycrystalline state (Fig. 4(a)). Doped films should also have a lower density of surface defects due to the larger grain size. However, some authors found a decrease in fracture strength with doping.^(25,35) This decrease can be explained by additional surface defects generated by surface oxidation.

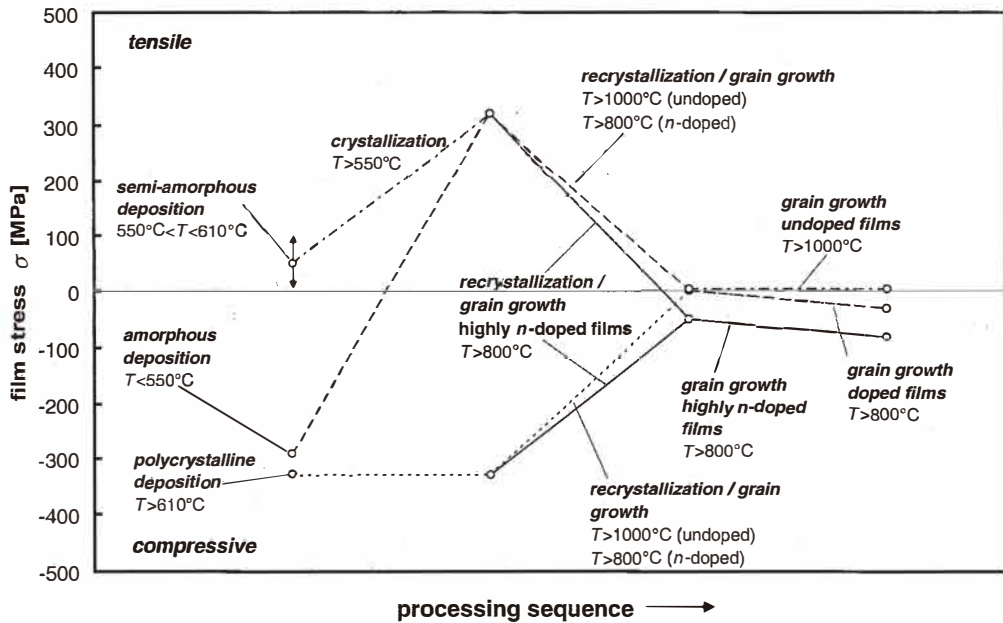


Fig. 9. Change of polysilicon film stress by phosphorus doping and subsequent annealing. The stress values for 1 μm thick films are determined from wafer-bow measurements (accuracy 5 MPa).

3.5 Postprocessing

As recrystallization and grain growth can continue in all postdoping high-temperature processing steps, the whole thermal budget following polysilicon doping has to be taken into account in investigating mechanical film properties. In highly *n*-type doped films, changes in mechanical characteristics are already observed at temperatures above 800°C.

4. Conclusions

The mechanical properties of thin polycrystalline silicon films are significantly affected by deposition, doping and subsequent annealing processes. It was shown that the elastic properties are mainly determined by preferred grain orientation. The lowest Young's modulus and Poisson's ratio are expected for films with randomly oriented grains. This is the case in films that are deposited in the amorphous form and subsequently crystallized. Randomly oriented grains are also found in films that are recrystallized due to doping and annealing.

Film stress and intrinsic bending moments are found to be defined by grain boundary formation and, for amorphously deposited films, the density change during amorphous to crystalline state transition. By detailed stress profile measurements, the connection of film stress to microstructure has been confirmed. Stress relaxation due to recrystallization

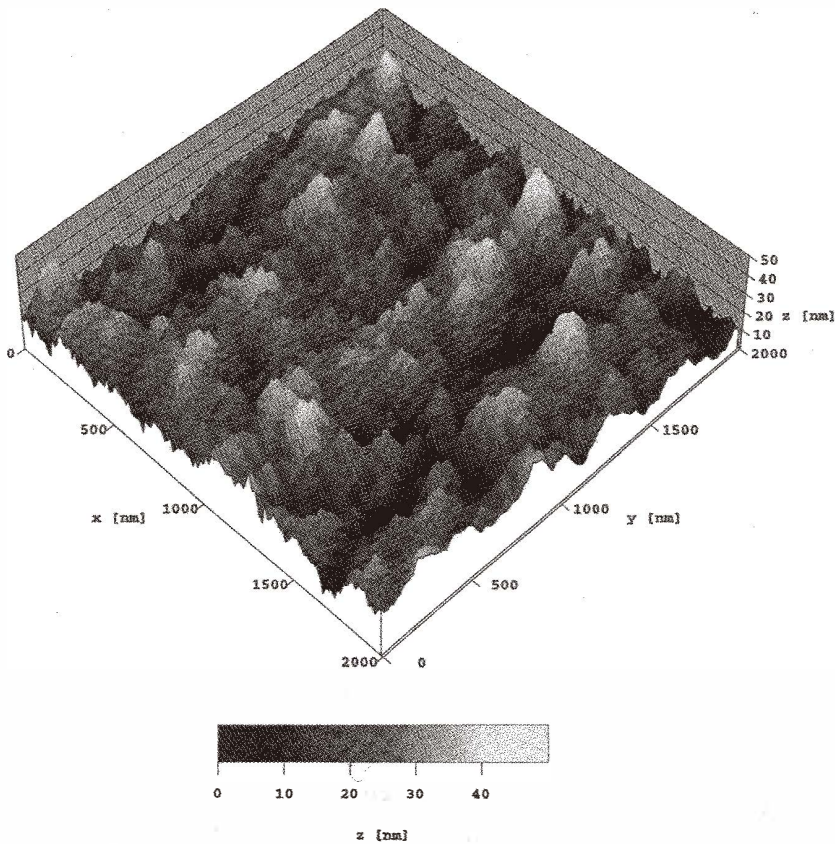


Fig. 10. Surface roughness of a doped polycrystalline silicon films measured by AFM. The film was deposited at 620°C and subsequently diffusion doped at 950°C using POCl_3 .

processes is found to be the major effect of doping on film stress. An additional compressive stress contribution is found in highly phosphorus-doped films.

The fracture strength of thin polysilicon films is seen to depend mainly on the density of surface defects, i.e. surface roughness. The smoothest surface is found for polycrystalline films deposited amorphously at low temperatures, having a fracture strength near the value of single crystalline silicon.

From these results, an optimized processing sequences for the fabrication of polysilicon films for micromechanical applications can be deduced: The chosen deposition temperature should be as low as possible, with a deposition rate that is still acceptable. The film should then be crystallized in a postdeposition annealing step. Thus, tensile films with a low intrinsic bending moment and a high fracture toughness are fabricated. With respect to

sheet resistivity, the doping process should be conducted with special attention given to maintain a uniform (or, at least, symmetrical) dopant concentration throughout the thickness of the film to preserve the low intrinsic bending moment. Dopant concentration and annealing temperature should be moderate to avoid substantial recrystallization and grain growth. These would decrease the fracture strength and may generate compressive film stress. *p*-Type dopants are preferable when high dopant concentrations are necessary. Oxidizing ambients may have severe consequences on polysilicon film stress and fracture toughness and thus should be avoided.

As an example of the implementation of the above described processing rules, the development of a phosphorus-doped polysilicon film with low tensile stress and a low intrinsic bending moment is shown in Figs. 11 to 13. The 1- μm -thick polysilicon film is deposited in two 500 nm steps at 585°C. Each layer of the film is crystallized at 650°C immediately after deposition and subsequently doped by ion implantation. The implantation energy is optimized to produce a symmetric doping profile (Fig. 11). After the subsequent annealing for 1 h at temperatures between 850°C and 1,050°C, a near-zero film stress and stress gradients down to 5 MPa/ μm were observed (Figs. 12 and 13).

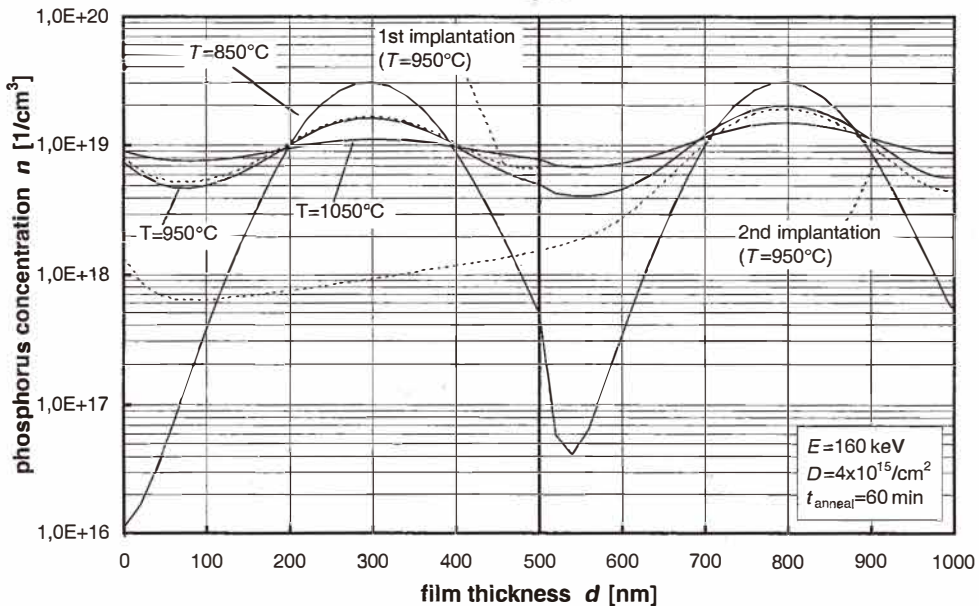


Fig. 11. Simulated concentration profile of phosphorus in two stacked 500-nm-thick polysilicon films that were deposited and ion-implanted one after the other. The curves are calculated for three different annealing temperatures: 850°C, 950°C and 1,050°C. For comparison, the doping profiles of the single implantations are also shown (only for $T = 950^\circ\text{C}$).

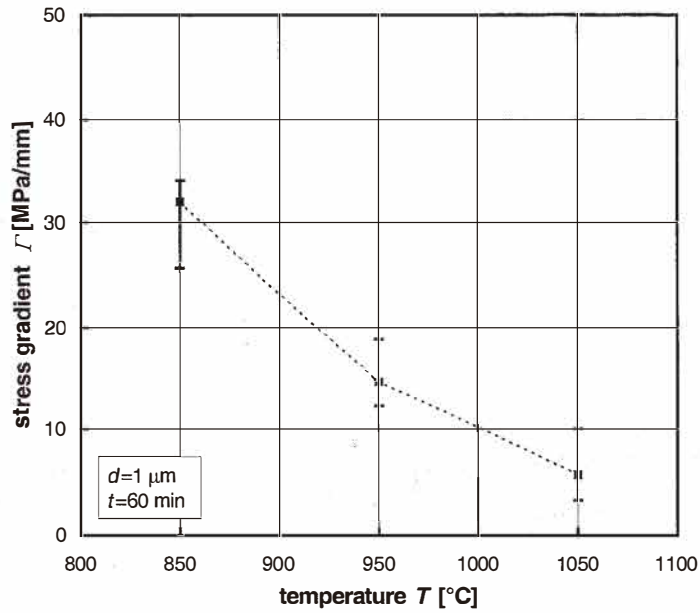


Fig. 12. Measured stress gradient in the double ion-implanted polysilicon films after annealing at three different annealing temperatures. The error bars depict the variation of stress gradient on a single 4" wafer.

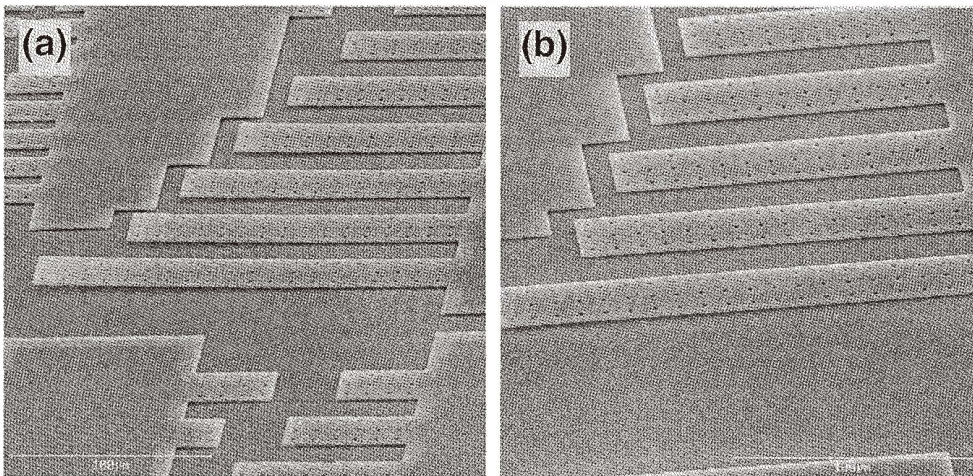


Fig. 13. Free standing cantilever beams up to 200 μm in length indicating the low intrinsic bending moment for the double ion-implanted 1- μm -thick polysilicon film annealed at (a) 850°C and (b) 1,050°C.

References

- 1 K. E. Petersen: *Proc. IEEE* **70** (1982) 420.
- 2 R. T. Howe and R. S. Muller: *Electrochem. Soc. Meeting Ext. Abstracts Vol. 82-1* (Montreal, Canada, 1982) p. 184.
- 3 R. T. Howe and R. S. Muller: *J. Electrochem. Soc.* **130** (1983) 1420.
- 4 H. C. Nathanson and R. A. Wickstrom: *Appl. Phys. Lett.* **7** (1965) 84.
- 5 T. A. Core, W. K. Tsang and S. J. Sherman: *Solid State Technology Oct.* (1993) 39.
- 6 M. Offenbergl, F. Lärmer, B. Elsner, H. Münzel and W. Riethmüller: *Tech. Dig. 8th Int. Conf. on Solid-State Sensors and Actuators, Transducers '95* (Stockholm, Sweden, 1995) p. 589.
- 7 H.-J. Timme, D. Draxelmayer, C. Hierold, S. Kolb, D. Maier-Schneider, E. Pettepaul, T. Scheiter, M. Steger and W. M. Werner: *Proc. Sensor 97 Congress*, (Nuernberg, Germany, 1997) p. 65.
- 8 H. Guckel, D. W. Burns, C. C. G. Visser, H. A. C. Tilmans and D. DeRoo: *IEEE Transactions on Electron Devices* **35** (1988) 800.
- 9 P. J. French, B. B. van Drieënhuizen, D. Poenar, J. F. L. Goosen, R. Mallée, P. M. Sarro and R. F. Wolffenbuttel: *J. of Microelectromechanical Systems* **5** (1996) 187.
- 10 L. Elbrecht, R. Catanescu, J. Zacheja and J. Binder: *Sensors and Actuators A* **61** (1997) 374.
- 11 D. O. King, M. C. L. Ward, K. M. Brunson and D. J. Hamilton: *Sensors and Actuators A* **68** (1998) 238.
- 12 T. I. Kamins: *J. Electrochem. Soc.* **127** (1980) 686.
- 13 T. I. Kamins: *Polycrystalline silicon for integrated circuit applications* (Kluwer Academic Publishers, Boston, 1988).
- 14 R. Bisaro, J. Magarino, N. Proust and K. Zellama: *J. Appl. Phys.* **57** (1986) 1167.
- 15 D. Meakin, J. Stoemenos, P. Migliorato and N. A. Economou: *J. Appl. Phys.* **61** (1987) 5031.
- 16 T. I. Kamins: *Sensors and Actuators A* **21-23** (1990) 817.
- 17 P. Krulevitch, T. D. Nguyen, G. C. Johnson, R. T. Howe, H. R. Wenk and R. Gronsky: *Proc. Mater. Res. Soc. Vol.* **202** (1991) p. 167.
- 18 P. Krulevitch, G. C. Johnson and R. T. Howe: *Proc. Mat. Res. Soc. Vol.* **239** (1992) p. 13.
- 19 W. A. Brantley: *J. Appl. Phys.* **44** (1973) 534.
- 20 R. Hill: *Proc. Phys. Soc.* **A65** (1952) 351.
- 21 J. Imhof: *Zeitschrift für Metallkunde* **66** (1975) 227.
- 22 D. Maier-Schneider, A. Köprülü, S. Ballhausen Holm and E. Obermeier: *J. Micromech. Microengineering* **6** (1996) 436.
- 23 L. Elbrecht, U. Storm, R. Catanescu and J. Binder: *J. Micromech. Microengineering* **7** (1997) 151.
- 24 O. Tabata, S. Sugiyama and M. Takigawa: *Appl. Phys. Lett.* **56** (1990) 1314.
- 25 J. A. Walker, K. J. Gabriel and M. Mehrengany: *J. Electronic Materials* **20** (1991) 665.
- 26 J. Koskinen, E. Steinwall, R. Soave and H. H. Johnson, *J. Micromech. Microengineering* **3** (1993) 13.
- 27 R. I. Pratt, G. C. Johnson, R. T. Howe and J. C. Chang: *Tech. Dig. 6th Int. Conf. on Solid-State Sensors and Actuators, Transducers '95* (Stockholm, Sweden, 1995) p. 205.
- 28 W. N. Sharpe, B. Yvan, R. L. Edwards and R. Vaidyanathan: *Proc. IEEE Int. Workshop on Micro Electro Mechanical Systems, MEMS '97* (Nagoya, Japan, 1997) p. 424.
- 29 H. Guckel, J. J. Sniegowski, T. R. Christenson, S. Mohny and T. F. Kelly: *Sensors and Actuators* **20** (1989) 117.
- 30 D.-G. Oei and S. L. McCarthy: *Proc. Mat. Res. Soc. Symp. Vol.* **276** (1992) p. 85.
- 31 A. Benítez, J. Bausells, E. Cabruja, J. Esteve and S. Samitier: *Sensors and Actuators A* **37-38** (1993) 723.

- 32 P. A. Krulevitch: Micromechanical Investigations of Silicon and Ni-Ti-Cu thin films (Ph. D. Dissertation, University of California, Berkeley, USA, 1994).
- 33 T. I. Kamins: *J. Electrochem. Soc.* **121** (1974) 681.
- 34 T. Tsuchiya, O. Tabata, J. Sakata and Y. Taga: Proc. IEEE Int. Workshop on Micro Electro Mechanical Systems, MEMS '97 (Nagoya, Japan, 1997), p. 529.
- 35 M. Biebl and H. v. Philipsborn: Tech. Dig. 8th Int. Conf. on Solid-State Sensors and Actuators, Transducers '95, (Stockholm, Sweden, 1995) p. 72.
- 36 S. Greek, F. Ericson, S. Johansson and J.-Å. Schweitz: *Thin Solid Films* **292** (1997) 247.
- 37 C. P. Chen and M. H. Leipold: *American Ceramic Society Bulletin* **59** (1980) 469.
- 38 S. M. Hu: *J. Appl. Phys.* **53** (1982) 3567.
- 39 F. Ericson and J.-Å. Schweitz: *J. Appl. Phys.* **68** (1990) 5840.
- 40 C. J. Wilson, A. Ormeggin and M. Nabutovskih: *J. Appl. Phys.* **79** (1996) 2386.
- 41 Y. B. Gianchandani, M. Shinn and K. Najafi: Tech. Dig. Int. Conf. on Solid-State Sensors and Actuators, Transducers '97 (Chicago, USA, 1997) p. 623.
- 42 Y. Wada and S. Nishimatsu: *J. Electrochem. Soc.* **125** (1978) 1499.
- 43 L. Mei, M. Rivier, Y. Kwarck and R. W. Dutton: *J. Electrochem. Soc.* **129** (1982) 1791.
- 44 T. A. Arias, and J. D. Joannopoulos: Proc. 3rd Int. Symp. on Process Physics and Modeling in Semiconductor Technology (Honolulu, Hawaii, 1991) p. 403.
- 45 F. S. Becker, H. Oppolzer, I. Weitzel, H. Eichmüller and H. Schaber: *J. Appl. Phys.* **56** (1984) 1233.
- 46 S. J. Krause, S. R. Wilson, W. M. Paulson and R. B. Gregory: Proc. Mater. Res. Soc. Vol. **35** (1985) p. 721.
- 47 M. Orpana and A. O. Korhonen: Tech. Dig. 6th Int. Conf. on Solid-State Sensors and Actuators, Transducers '91 (San Francisco, USA, 1991) p. 957.
- 48 H.-J. Kim and C. V. Thompson: *Appl. Phys. Lett.* **48** (1986) 399.
- 49 D. T. Read and J. C. Marshall: Proc. SPIE Vol. **2880** (1996) p. 56.
- 50 R. K. Gupta, P. M. Osterberg and S. D. Senturia: Proc. SPIE Vol. **2880** (1996) p. 39.
- 51 R. I. Hegde, W. M. Paulson and P. J. Tobin: *J. Vac. Sci. Technol. B* **13** (1995) 1434.